Time–Temperature Dependency of Mode II Fracture Toughness for Bisphenol A Type Epoxy Resin

Wakako Araki, Daisuke Asahi, Tadaharu Adachi, Akihiko Yamaji

Department of Mechanical Sciences and Engineering, Tokyo Institute of Technology, 2-12-1 Ookayama, Meguro-ku, Tokyo 152-8552, Japan

Received 1 June 2004; accepted 2 September 2004
DOI 10.1002/app.21358
Published online 26 January 2005 in Wiley InterScience (www.interscience.wiley.com).

ABSTRACT: We investigated the mode II fracture toughness (K_{IIc}) with time and temperature dependence of the bisphenol A type of epoxy resin. We performed an asymmetric four-point bending test under various conditions of temperature and displacement rate. We found that K_{IIc} strongly depended on the displacement rate and the temperature, even at room temperature. Moreover, it was governed by the time–temperature equivalence principle in regard to the fracture time. The time–temperature dependency of K_{IIc} was similar to that of the loss modulus (E''), and the transition of brittle to ductile fractures occurred nearly simultaneously when E'' peaked. © 2005 Wiley Periodicals, Inc. J Appl Polym Sci 96: 51–55, 2005

Key words: fracture; thermal properties; viscoelastic properties; resins

INTRODUCTION

Epoxy resin is widely used in various engineering fields because of its excellent mechanical properties, good electrical insulation, and strong adhesion to other materials. As epoxy resin is used over a wide range of temperatures, the estimation of the temperature dependence of its mechanical properties, such as the fracture toughness, is very important.

Epoxy resin is a thermoviscoelastic material. Its strength depends on not only temperature but also time because of its thermoviscoelastic nature. Both temperature and time dependencies must be taken into account according to the time–temperature equivalent principle. The yield stress, strength, and viscoelastic properties have the same equivalent factor, which is called the shift factor (a_T). Recent studies[1–4] of the resin's mode I (tensile) fracture toughness (K_{Ic}) have shown that it strongly depends on both time and temperature and has the same a_T as the viscoelastic properties.

Most of studies on mode II (in plane shear) fracture toughness (K_{IIc}) have dealt with composite laminates.[5–7] The interlaminar K_{IIc} of the laminates has been conventionally examined by end-notched flexible or end-notched shearing tests. Few studies of on K_{IIc} of bulk epoxy resin have been reported.[8,9] Moreover, the time–temperature dependency of K_{IIc} of the epoxy resin has not yet been clarified.

Correspondence to: W. Araki (araki@mech.titech.ac.jp).

Journal of Applied Polymer Science, Vol. 96, 51–55 (2005)

In previous studies,[3,4] we clarified the time–temperature dependence of K_{Ic} for bisphenol A type epoxy resin and its composites. The purpose of this study was to clarify the time–temperature dependency of K_{IIc} for bisphenol A type epoxy resin.

EXPERIMENTAL

Specimens

The epoxy resin used in the experiment was a blend of bisphenol A type epoxide resin (Japan Epoxy Resins Co., Ltd., Epikote 828, Japan) with metyltetrahydrophthalic anhydride as a curing agent (Hitachi Chem, HN-2200R, Japan) and 2,4,6-tris(dimethylaminomethyl) phenol (Daito Curar, DMP-30, Japan) as an accelerator. The weight ratio of the resin, curing agent, and accelerator was 100:80:0.5, which was determined by the measurement of the heat deformation temperature. The mixture of raw materials was cast in a mold after it was agitated and degassed *in vacuo* and was then cured in a thermostatic oven. The curing was performed in two steps. First, for precuring, the specimen was kept at 353 K for 3 h to gel the matrix resin. Then, for postcuring, which affected the crosslinking reaction of the resin, the specimen was kept at 433 K for 15 h.

Measurement of thermoviscoelasticity

We measured the specimen's dynamic storage modulus (E') and dynamic loss modulus (E'') with a dynamic viscoelastometer (Orientec, Rheovibron DDV-III-EA, Japan). Tensile vibrations at 3.5, 11, 35, and 110

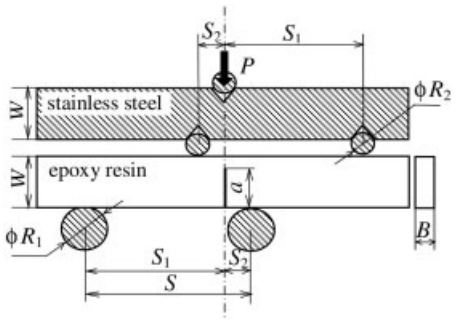

Figure 1 Asymmetric four-point bending test.

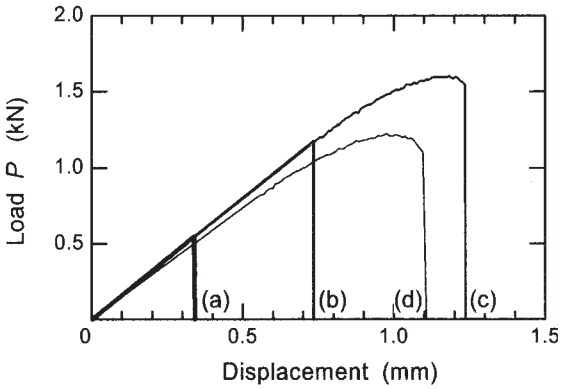

Figure 2 Load displacement curve: displacement rate = 1 μm/s and temperature = (a) 253, (b) 298, (c) 323, and (d) 348 K.

Hz were applied to the specimen every 2 K from 123 to 523 K. The master curve of E' was derived from its temperature dependence curves shifted along the frequency axis with a a_T in accordance with the time–temperature equivalence principle. Then, we derived the glass-transition temperature from the results of a thermoviscoelasticity measurement of each specimen to evaluate the degree of the curing reaction.[10]

K_{IIc} test[11]

We conducted an asymmetric four-point bending test of a precracked specimen to measure K_{IIc}. The geometry and the size of the specimens are shown in Figure 1 and Table I, respectively. For $a/W \approx 0.75$ (where a and W are defined in Fig. 1) in this test, a stress field around a crack tip became pure in-plane shearing and that induced mode II fracture behavior.

The tests were conducted with a universal material testing machine (Instron 8501, Instron, Canton, MA) under various constant displacement rates from 1 to 30 μm/s at the loading point, at different temperatures from 123 to 348 K in a thermostatic oven (Instron 3119-007, Instron). We performed the tests to investigate the temperature and time dependence of K_{IIc}. We measured the histories of the load and displacement at the loading point. We calibrated the displacement on the basis of measured local deformations of the epoxy specimen and confirmed that the deformation of the stainless steel jig could be neglected.

If the load displacement curve of each specimen is almost linear until breaking, the stress field near the crack tip is regarded as small scale yielding. Therefore, linear elastic fracture mechanics can be applied to determine fracture toughness. The stress intensity factor for mode II (K_{II}) is given by[11]

$$K_{II} = F_{II}(\alpha)\tau\sqrt{\pi a} \tag{1}$$

where

$$F_{II}(\alpha) = -0.2915 + 6.3229\alpha - 9.1199\alpha^2 + 6.0570\alpha^3$$

$$\tau = \frac{P_1 - P_2}{WB}$$

$$P_1 = \frac{S_1}{S}P, \quad P_2 = \frac{S_2}{S}P,$$

$$\alpha = \frac{a}{W}$$

where P, S, S_1, S_2, W, B, and a are defined in Figure 1. Substituting the maximum load at fracture into P in eq. (1) determines K_{IIc}.

After the fracture toughness test, we observed the fractured surfaces with an optical microscope (SZH-ILLD, Olympus Optical, Japan) and a scanning electron microscope (JSM-T200, Jeol, Japan) at an accelerating voltage of 5 kV.

TABLE I
Sizes (mm) for the Asymmetric Four-Point Bending Test

S	S_1	S_2	W	B	a	R_1	R_2
36	30	6	12	5	9	10	5

All variables are defined in Figure 1.

RESULTS AND DISCUSSION

Load displacement curve

Figures 2 shows typical load displacement curves of the specimens at a rate of 1 μm/s under various temperature conditions. Whenever the temperature was less than 298 K, the load displacement curves were linear until fracture. The slopes were almost the same, and the maximum load increased with the temperature. At 323 K, the maximum load became larger, and the curve exhibited a slightly nonlinear relation just before brittle fracture due to insufficient ductility.

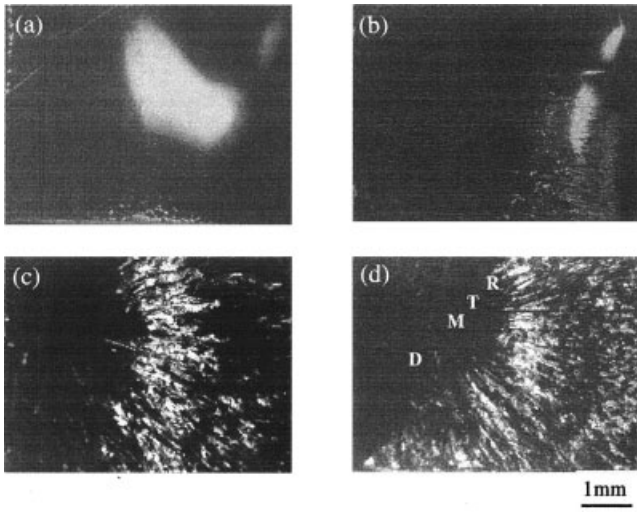

Figure 3 Fractured surface observed with an optical microscope. (the initial crack existed at the far left, and the crack propagated from left to right, as shown in each picture): displacement rate = 1 μm/s and temperature = (a) 253, (b) 298, (c) 323, and (d) 348 K (D = ductile crack propagation; M = mirror-like region; T = transition region from mirror-like to rough surface; R = rough region.)

The curve for 348 K denoted a more nonlinear relationship, and the maximum load was smaller than that for 323 K. Hereafter, we call such a brittle fracture accompanied with slightly nonlinear stiffness, such as the cases at 323 and 348 K, *quasibrittle fractures*.[12] Whenever temperature was more than 348 K, a ductile fracture occurred for any displacement rate within these experimental conditions. In this study, the K_{IIc} values were evaluated from the maximum value of each load displacement curve according to eq. (1) for brittle and quasibrittle fractures.

Fractography

The overall features of the fractured surface as observed with the optical microscope are shown in Figure 3, where each specimen corresponds to that used to obtain the results shown in Figure 2.

The typical features for brittle fracture[10,13,14] are shown in Figure 3(a,b). Figures 3(a) and 3(b) both show a smooth, mirror-like surface near the initial crack tip. As the crack propagated, pits began to appear on the surfaces and developed into parabolic patterns so that the surfaces gradually became rough. As the crack propagated further, the parabolic patterns superimposed, and the surface became rougher. The surface of the specimen tested at 298 K was rougher than that at 253 K when the maximum load at 298 K was larger than that at 253 K, as shown in Figure 2.

Figure 3(c,d) shows quasibrittle fracture. Figure 4 presents the details of Figure 3(d), as observed with

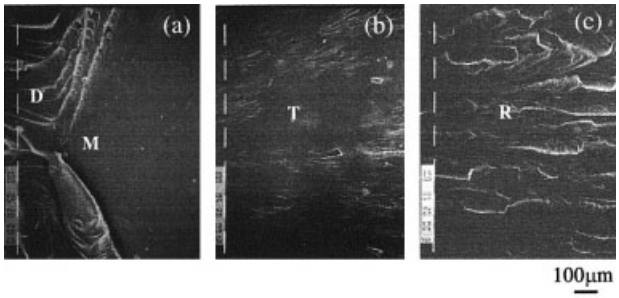

Figure 4 Fractured surface observed with a scanning electron microscope [the initial crack existed at the far left, as shown in part (a), and the crack propagated from left to right, as shown in each picture]: displacement rate = 1 μm/s and temperature = 348 K. (a) Ductile crack propagation (D) and mirror-like regions (M), (b) transition region from mirror-like to rough surface (T), and (c) rough region (R).

the scanning electron microscope. The ductile crack propagation[15] appeared near the initial crack tip before a mirror-like surface. [see Fig. 4(a)]. After that, as was the case with the brittle fracture, the pits on the smooth surface developed into the parabolic patterns shown in Figure 4(b). These parabolic patterns superposed, and then, the surface became rough, as shown in Figure 4(c). The region of the ductile crack propagation at 348 K was larger than that at 323 K when the maximum load at 348 K was smaller than that at 323 K, as shown in Figure 2.

K_{IIc} with temperature and time dependence

Figure 5 shows the temperature dependency of K_{IIc} under various rate conditions. At fast displacement rates, 10 and 30 μm/s, K_{IIc} was small at lower temperatures and gradually increased with the tempera-

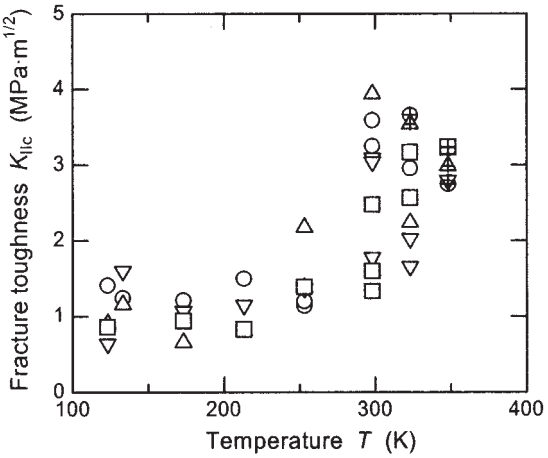

Figure 5 K_{IIc} with temperature dependence. Displacement rate: (○) 3.5, (△) 11, (▽) 35, and (□) 110 Hz (a + with a shape represents a quasibrittle fracture, e.g., ⊕ means that a specimen tested at 3.5 Hz fractured quasibrittlely).

ture up to 348 K. The quasibrittle fracture appeared around at 348 K, and then, the fracture form transferred from brittle to ductile. At slower rate conditions of 1 and 3 μm/s, K_{IIc} was small at lower temperatures and increased with temperature up to 298 K. Then, the quasibrittle fracture appeared at 323 K, and K_{IIc} decreased with temperature. K_{IIc} was less than 2.0 MPa·m$^{1/2}$ at any temperatures less than 253 K regardless of the rate conditions, although the values at 298 and 323 K were greatly scattered from 1.0 to 4.0 MPa·m$^{1/2}$. At 348 K, K_{IIc} was almost 3.0 MPa·m$^{1/2}$

Figure 6 shows the relationship between K_{IIc} and the fracture time (t_f). t_f denotes the duration of loading until brittle fracture. K_{IIc} increased with t_f under any temperature conditions except 348 K. For 348 K, when a quasibrittle fracture occurred in all the specimens, K_{IIc} slightly decreased with t_f. Thus, we found that K_{IIc} greatly depended on both temperature and time (or rate).

Master curve of K_{IIc}

To summarize the aforementioned dependencies of K_{IIc}, we made the master curves of the K_{IIc} data with a_T derived from the time–temperature dependence of E'. t_f was used as the time parameter instead of the displacement rate.[3,4] The master curve of K_{IIc} with regard to reduced time (ξ) compared with E' and E'' at the standard temperature of 298 K is shown in Figure 7. As shown in Figure 7(a), E' decreased gradually as the reduced time increased to 10^5 s and then sharply decreased. E'' exhibited a small peak around 10^{-5} s and, after that, increased until about 10^5 s, where it peaked fully. After 10^5 s, E'' decreased sharply. An α-relaxation phenomena was seen at 10^5 s in both E' and E''.

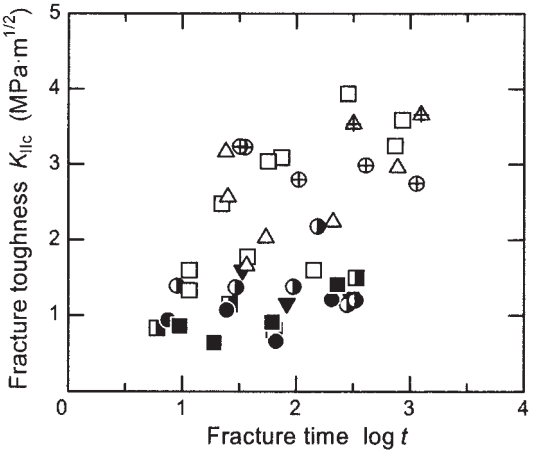

Figure 6 K_{IIc} with t_f dependence. Temperature: (■) 123, (▼) 133, (●) 173, (◧) 213, (◐) 253, (□) 298, (△) 323, and (○) 348 K (a + with a shape represents a quasibrittle fracture, e.g., ⊕ means that a specimen tested at 348 K fractured quasibrittlely.)

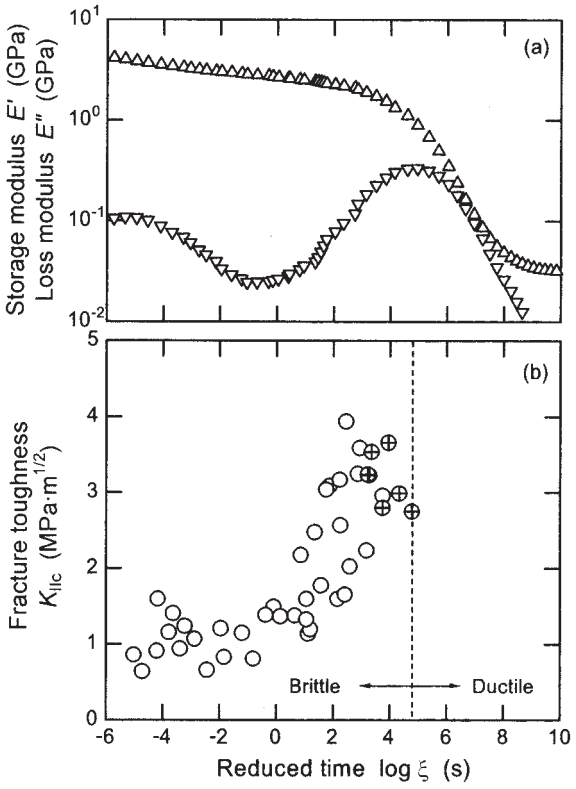

Figure 7 Master curves of dynamic moduli and K_{IIc} (standard temperature = 298 K): (a) dynamic moduli [(△) E' and (▽) E''] and (b) K_{IIc} (a + represents a quasibrittle fracture).

As shown in Figure 7(b), K_{IIc} was approximately 1.0 MPa·m$^{1/2}$ near 10^{-2} s. K_{IIc} increased drastically for the time being. After that, a quasibrittle fracture appeared, K_{IIc} hit a maximum value of about 3.5 MPa·m$^{1/2}$ around 10^4 s, and then, a ductile fracture appeared from 10^5 s. The variation of K_{IIc} was also caused by the relaxation phenomena. The increase in K_{IIc} seemed to be similar to that in E'', and the brittle-to-ductile fracture transition appeared near the peak of E'' ($\xi = 10^5$ s).

Compared with K_{Ic},[3,4] the time of a brittle–ductile fracture transition in K_{IIc} was almost the same as the maximum time of E'', although K_{Ic} had its brittle–ductile transition when E'' had not peaked yet. Moreover, the behavior of K_{IIc} was really variable, even at room temperature, although K_{Ic} was almost constant under the same conditions. Some studies have reported[8,9] various values of K_{IIc}. Also, it was pointed out that the evaluation of K_{IIc} is essentially difficult, although many methods and techniques for this evaluation have been examined.[16,17] The significant time–temperature dependence of K_{IIc} could make its value unstable and cause difficulty in measuring it at room temperature.

CONCLUSIONS

We investigated K_{IIc} with time and temperature dependence of a bisphenol A type of epoxy resin. We

performed an asymmetric four-point bending test under various conditions of temperature and displacement rate.

We found that K_{IIc} strongly depended on the displacement rate and the temperature, even at room temperature. Moreover, it was governed by the time–temperature equivalence principle in regard to t_f. The time–temperature dependency of K_{IIc} was similar to that of E'', and the transition of brittle to ductile fractures occurred nearly simultaneously when E'' peaked.

References

1. Popelar, S.; Chengalva, M. K.; Popelar, C. H.; Kenner, V. H. Time-Dependent Failure of Polymers: Experimental Study; Kenner, V. H., Ed.; American Society of Mechanical Engineers: New York, 1992; p 15.
2. Adachi, T.; Iketaki, T.; Gamou, M.; Yamaji, A. Time–Temperature Dependence of Fracture Toughness for Bisphenol A Epoxy Resin: Proceedings of the 4th International Congress on Thermal Stresses; Osaka, 2001; p 65.
3. Araki, W.; Adachi, T.; Gamou, M.; Yamaji, A. Proc Inst Mech Eng Part L: J Mater Design Appl 2002, 216, 79.
4. Araki, W.; Adachi, T.; Yamaji, A. Mater Sci Forum 2003, 426–432, 1985.
5. Wang, W. X.; Takao, Y.; Matsubara, T.; Kim, H. S. Comp Sci Tech 2002, 62, 767.
6. Singh, S.; Partridge, I. K. Comp Sci Tech 1995, 55, 319.
7. Blackman, B. R. K.; Dear, J. P.; Kinloch, A. J.; MacGillivray, H.; Wang, Y.; Williams, J. G.; Yayla, P. J Mater Sci 1996, 31, 4467.
8. Kim, H. S.; Ma, P. J Appl Polym Sci 1998, 69, 405.
9. Liu, C.; Huang, Y.; Stout, M. G. Acta Mater 1998, 46, 5647.
10. Araki, W.; Adachi, T.; Yamaji, A.; Gamou, M. J Appl Polym Sci 2002, 86, 2266.
11. Stress Intensity Factors Handbook; Murakami, Y., Ed.; Pergamon: Oxford, England, 1987; p 941.
12. Adachi, T.; Osaki, M.; Yamaji, A.; Gamou, M. Proc Inst Mech Eng Part L: J Mater Design and Appl 2003, 217, 29.
13. Plangsangmas, L.; Mecholsky, J. J., Jr.; Brenman, A. B. J Appl Polym Sci 1999, 72, 257.
14. d'Almeida, J. R. M.; Menezes, G. W.; Monteiro, S. N. Mater Res 2003, 6, 415.
15. Gaymans, R. J.; Hamberg, M. J. J.; Inberg, J. P. F. Polym Eng Sci 2000, 40, 256.
16. Shetty, D. K.; Rosenfield, A. R.; Duckworth, W. H. Eng Frac Mech 1987, 26, 825.
17. Suresh, S.; Shih, C. F.; Morrone, A.; O'Dowd, N. P. J Am Ceram Soc 1990, 73, 1257.